ARTICLES

Inverse-square potential and the quantum vortex

Hua Wu and D. W. L. Sprung
Department of Physics and Astronomy, McMaster University, Hamilton, Ontario, Canada L8S 4M1
(Received 13 October 1993)

The vortex structure of the steady-state probability flow for a general one-particle system in quantum mechanics is introduced and its relationship to the inverse-square potential is discussed. The relationship is made clear by classifying the corresponding solutions of the related classical inverse-square-potential problem.

PACS number(s): 03.65.−w, 73.20.Dx, 47.10.+g, 74.20.−z

I. INTRODUCTION

Recently, in studying the patterns of quantum probability flow, we pointed out the important role of two special situations: the velocity node and the quantum vortex [1]. We argued that these two patterns are the keys to understanding the global probability flow problem. Of the two, the quantum vortex is particularly interesting. We related the number of quantum vortices to the action along a closed path and the enclosed magnetic flux, which may be viewed as a generalization of flux quantization. The key theoretical tool is the concept of "quantum potential" due to Bohm [2,3] in which the dynamics of the quantum probability flow is turned into a classical fluid problem involving an additional potential of quantum nature. The same form of potential also appeared in the theory of superconductivity, for example, see the *Feynman Lectures on Physics* [4], but there it played no great role.

Another interesting aspect of the quantum vortex is that it is strongly correlated with the classical inverse-square-potential problem. The inverse-square problem is solvable, and is discussed extensively in the literature on many-particle one-dimensional quantum systems [5–9]. It is interesting that such a useful potential arises in a quite different context where it is responsible for the formation of quantum vortices.

The theme of this paper is to discuss in detail the relationship between the inverse square potential and the quantum vortex. Section II derives the inverse-square quantum potential for a particle in a scalar plus vector potential near a wave function node. Section III then solves the classical inverse-square problem in two-dimensional space, particularly for the only possible closed orbit, which is a circle. Section IV gives a relationship derived from the properties of quantum vortices between the action integrated around a closed path, the flux through it, and any enclosed vortex. Section V discusses the quantum vortex in three-dimensional space. The related inverse-square classical problem is given in Appendix A. Finally, the conclusions are given in Sec. VI.

II. THE INVERSE-SQUARE QUANTUM POTENTIAL

Consider a quantum steady state for a pointlike particle of charge q in a vector potential $\mathbf{A}$ and scalar potential V. The time-independent Schrödinger equation is

$$\left[\left(\frac{\hbar}{i}\nabla - q\mathbf{A}\right)^2/(2m) + V\right]\psi = E\psi \quad . \tag{1}$$

Expressing ψ in terms of the probability density ρ and action S,

$$\psi = \sqrt{\rho}e^{iS/\hbar} \quad , \tag{2}$$

and substituting into the complex Schrödinger equation, we arrive at two real equations:

$$E = \frac{1}{2}m\mathbf{v}^2 + V - \frac{\hbar^2}{2m}\frac{\nabla^2\sqrt{\rho}}{\sqrt{\rho}} \tag{3}$$

and

$$\nabla\cdot\mathbf{j} = \nabla\cdot(\rho\mathbf{v}) = 0 \quad , \tag{4}$$

where

$$\mathbf{v} = (\nabla S - q\mathbf{A})/m \, . \tag{5}$$

Equation (4) is the equation of continuity for the steady state, as $\mathbf{j}$ is the probability current density. In fluid mechanics, the current density is the density times velocity, so $\mathbf{v}$ is interpreted as the velocity of a particle. With this interpretation, Eq. (3) is the law of conservation of energy for a particle in the external potential V plus a "quantum potential [2–4]"

$$Q \equiv -\frac{\hbar^2}{2m}\frac{\nabla^2\sqrt{\rho}}{\sqrt{\rho}} \, . \tag{6}$$

The classical equation of motion is obtained by taking the gradient of Eq. (3):

$$m\frac{d\mathbf{v}}{dt} = q\mathbf{v}\times\mathbf{B} - \nabla(V+Q) \quad , \tag{7}$$

where we have used $\partial\mathbf{v}/\partial t = 0$ for steady flow.

We would like to study the vorticity of the flow. From Eq. (5),

$$\nabla\times\mathbf{p} = \nabla\times(m\mathbf{v}) = \nabla\times\nabla S - q\mathbf{B} \ . \tag{8}$$

Obviously, a nonvanishing magnetic field supports vortices due to the Lorentz force. In order to study vortices of purely quantum nature, we must set $\mathbf{B} = 0$ temporarily. The first term in Eq. (8) is zero as long as S is nonsingular, in which case, the probability field is irrotational. This breaks down at points where $\rho = 0$, i.e., wave function nodes. At such points, S is not well defined, and the flow is singular. Since it is only at these points that the vorticity may be nonzero, the centers of the vortices, if any, must be at the wave function nodes. These are called quantum vortices.

At a node of the wave function, the probability density ρ is non-negative and continuous. An expansion of ρ starts at the second order. If we stop at the second order, the condition of non-negativity gives us a positive definite quadratic form. In terms of principal axis coordinates,

$$\rho = \sum_i X_i^2/a_i^2 \ . \tag{9}$$

Dimensionally, the dependence of ρ with $r = \sqrt{\sum_i X_i^2}$ is quadratic, so $\sqrt{\rho} \propto r$. The quantum potential derived from this has inverse-square radial dependence, $Q \propto 1/r^2$.

We shall first concentrate on the the two-dimensional case, writing

$$\rho = r^2(\cos^2\theta/a^2 + \sin^2\theta/b^2) \tag{10}$$

and

$$Q = -\frac{\hbar^2}{2m}\frac{a^2b^2}{(b^2\cos^2\theta + a^2\sin^2\theta)^2}\frac{1}{r^2} \equiv f(\theta)\frac{1}{r^2} \ . \tag{11}$$

In fact, Q will be an inverse-square potential as long as $|\psi|$ is a power of r. Figure 1 shows the wave function magnitude near one of the wave function nodes for an electron passing through a right-angle-bend waveguide [10–14]. The linearity of $|\psi|$ versus r is clear. If the potential is not symmetric with respect to the two principal axes, the lines of equal wave function magnitude become ellipses.

III. SOLUTION TO THE INVERSE-SQUARE PROBLEM

While Q is singular at $r = 0$, the external potential $V(x,y)$ can be ignored for small enough r. This gives rise to a Lagrangian

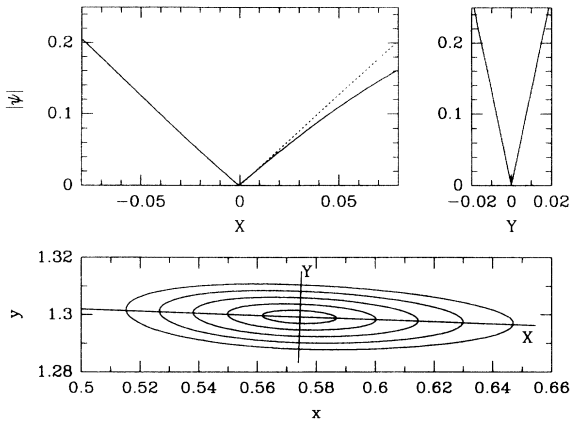

FIG. 1. Wave function magnitude near a wave function node for an electron passing a right-angle waveguide bend as shown in Fig. 2. The location of this node is indicated by a dashed box around the center of the second vortex counting from the upper lead. Bottom part: The equal wave function magnitude lines. Counting from the innermost ellipse, $|\psi| = 0.03, 0.06, \ldots$. As ψ increases, the curve starts to deviate from ellipses. Also drawn are the principal axes X and Y. Upper left part: $|\psi| \sim X$, this shows the linearity of $|\psi|$ versus r. The $X < 0$ and $X > 0$ parts are not exactly symmetric, the asymmetry increases as X increases. The dotted line is a mirror image of the $X < 0$ part, and it merges with the $X > 0$ part for small X. Upper right part: $|\psi| \sim Y$.

$$L = \frac{m}{2}(\dot{r}^2 + r^2\dot{\theta}^2) - \frac{f(\theta)}{r^2} \ , \tag{12}$$

which leads to equations of motion

$$m\ddot{r} = mr\dot{\theta}^2 + 2f(\theta)/r^3 \ , \tag{13}$$

$$\frac{d}{dt}(mr^2\dot{\theta}) = -f'(\theta)/r^2 \ . \tag{14}$$

It can be easily checked that these equations have a circular orbit solution $r = R$ for any R. We will now prove this to be a distinguishing feature of the inverse-square potential. Suppose a potential $V = V(r,\theta)$ supports circular orbits at any radius $r = R$, then

$$mR\dot{\theta}^2 = \left.\frac{\partial V}{\partial r}\right|_{r=R} \ , \tag{15}$$

$$mR^2\ddot{\theta} = -\left.\frac{\partial V}{\partial \theta}\right|_{r=R} \ . \tag{16}$$

Combining these two equations and eliminating $\dot{\theta}$ and $\ddot{\theta}$, $(R/2)[\partial^2 V/(\partial r\partial\theta)]_{r=R} = -[\partial V/\partial\theta]_{r=R}$ holds for any R, and thus

$$\frac{r}{2}\frac{\partial^2 V}{\partial r\partial\theta} = -\frac{\partial V}{\partial\theta} \ . \tag{17}$$

The general solution to this partial differential equation is

$$V = \frac{f(\theta)}{r^2} + g(r) \ . \tag{18}$$

Thus *an attractive two-dimensional potential supports*

circular orbits of arbitrary radius if and only if it can be written as the sum of a central potential and an inverse-square potential. Furthermore, if all the circular orbits have the same energy E, then $g(r) = E$. But why are we interested in studying circular orbits? What is the connection to the vortex? To answer this question, let us integrate the equations of the motion. Multiplying Eq. (14) by $r^2\dot{\theta}$, one has

$$\frac{d}{dt}\left[\frac{1}{2}mr^4\dot{\theta}^2 + f(\theta)\right] = 0\,. \tag{19}$$

Together with the energy conservation

$$E = \frac{1}{2}m(\dot{r}^2 + r^2\dot{\theta}^2) + \frac{f(\theta)}{r^2} \tag{20}$$

we see that

$$F = r^2\left(E - \frac{1}{2}m\dot{r}^2\right) \tag{21}$$

is a constant of the motion. The existence of this conserved quantity has profound consequences for our problem. Since streamlines do not cross each other, the orbits near the center of a quantum vortex must be closed. Any closed orbit has a maximum (r_{max}) and minimum (r_{min}) radius. At these extrema, $\dot{r} = (dr/d\theta)\dot{\theta} = 0$. From Eq. (21), $E(r_{max}^2 - r_{min}^2) = 0$. If $r_{max} = r_{min}$, the orbit is a circle. On the other hand, if $E = 0$, $F = -r_{max}^2 m\dot{r}^2/2 = 0$, and $\dot{r} = 0$. Therefore, *all closed orbits of a particle moving in an inverse-square potential are circles.* This immediately implies that *streamlines of a quantum vortex are circles for small r.* This conclusion is well verified in many examples of the electron waveguide problem [11–14].

Figure 2 shows some flow lines for an electron passing through a right-angle-bend waveguide. We see six quantum vortices in the region plotted. In the right upper corner of the figure is a magnification of the second vortex (counting from the upper entrance) in the dash box, showing that the flux lines are circles. In fact, by examining the energy of the particle, one finds that a circular orbit implies $E = F = 0$. But in our problem, the energy of the particle is given: why do we still see circular orbits? The answer lies in the singularity of the inverse potential; for small r, the potential is so large in magnitude that the energy of the particle can be neglected. On the other hand, the quantum potential we derived relies on the small r expansion of the probability density, which is nevertheless an approximation. From the observed circular orbits, it is reasonable to assume the quantum potential to be $Q = f(\theta)/r^2 + E$, which supports circular orbits at energy E.

We shall now classify the solutions to the inverse-square problem. Equation (21) implies $Er^2 - F \geq 0$. Solving for $\dot{r}$ from Eq. (21) gives an equation to determine $r(t)$:

$$\dot{r} = \pm\sqrt{\frac{2}{m}}\frac{\sqrt{Er^2 - F}}{r}\,. \tag{22}$$

The $\pm$ sign depends on whether the particle is leaving or approaching the center. With the help of energy conservation,

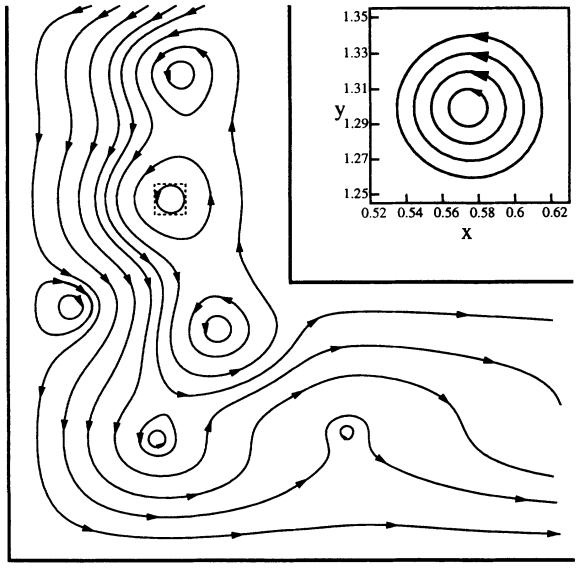

FIG. 2. Some stream lines for an electron passing a right-angle-bend waveguide without magnetic field. The electron energy is $E = 6.25E_1$, where E_1 is the first open mode threshold. The electron enters from the top left in the first transverse mode, and is transmitted to the lower right lead with a transmission probability 0.264. Six quantum vortices are shown. Some stream lines inside the dashed box for the second vortex (counting from the top) are magnified in the upper right corner to demonstrate that the the stream lines close to the center of a quantum vortex are circles.

$$r'^2[F - f(\theta)] = r^2[Er^2 - F]\,, \tag{23}$$

where $r' = (dr/d\theta)$. Since $Er^2 - F \geq 0$, $F - f(\theta) \geq 0$, and the equation to determine the orbit is

$$r' = \pm\frac{r\sqrt{Er^2 - F}}{\sqrt{F - f(\theta)}}\,. \tag{24}$$

All possible solutions may be listed as follows.

(a) $E < 0$: These orbits are bounded outward. Since $Er^2 - F > 0$, $F < 0$. Because E and F have the same sign, we can define $F = ER^2$ with R a positive number. By consulting Eq. (21), we see that R is the maximum of r. Integrating Eqs. (22) and (24) yields a radial integral:

$$r = \sqrt{|R^2 + (2E/m)t^2|} \tag{25}$$

and the orbit

$$r = \frac{R}{\cosh\int_{\theta_0}^{\theta}\frac{\sqrt{-F}d\theta}{\sqrt{F - f(\theta)}}}\,, \tag{26}$$

where $\theta_0 = \theta|_{t=0}$, and the origin of time is chosen when $r = R$ takes place. Combining the above two equations, we have an implicit angular integral

$$t = \pm R/\sqrt{-2E/m}\tanh\int_{\theta_0}^{\theta}\frac{\sqrt{-F}d\theta}{\sqrt{F - f(\theta)}}\,. \tag{27}$$

Supposing the particle to rotate in the anticlockwise direction, we pick up the positive sign. The motion of the particle is pictured as follows: At $t = -R/\sqrt{-2E/m}$, $\theta = -\infty$. It then spirals out and at $t = 0$, it reaches its maximum radius R. Passing this point, it spirals in, and reaches the center at $t = R/\sqrt{-2E/m}$, when $\theta = +\infty$. It could then start a new cycle with $\theta = -\infty$. However, this switch over at infinity introduces uncertainty into the problem, as the particle starting a new cycle by spiraling out forgets the history of how it spiraled in. So every new cycle is independent; it doesn't have to repeat the previous one. Within one cycle, the motion is deterministic, but in between cycles, the motion is random, i.e., θ_0 is a random variable of cycles.

(b) $E = 0$, $F = 0$: In this case, we have circular orbits $r = R$, where R is any positive number. Keeping $F = ER^2$, and taking the limit $E \to 0$, Eq. (27) is transformed into

$$t = \pm\sqrt{\frac{m}{2}}R^2 \int_{\theta_0}^{\theta} \frac{d\theta}{\sqrt{-f(\theta)}} . \tag{28}$$

(c) $E = 0$, $F \neq 0$: We shall call these noncircular zero energy orbits. From Eq. (21), $F < 0$. The radial integral, orbit, and angular integral are found to be

$$r = \sqrt{|R^2 \pm \sqrt{-8F/m}\, t|} , \tag{29}$$

$$r = R \exp\left(\pm \int_{\theta_0}^{\theta} \frac{\sqrt{-F}d\theta}{\sqrt{F - f(\theta)}} \right) , \tag{30}$$

and

$$t = \pm R^2\sqrt{-m/(8F)} \left[\exp\left(\pm 2 \int_{\theta_0}^{\theta} \frac{\sqrt{-F}d\theta}{\sqrt{F - f(\theta)}} \right) - 1 \right] , \tag{31}$$

where R is the initial value of r, not determined by E and F. Though apparently different from case (a), it can be deduced from (a) by shifting the origin of time and angle and taking the limit $E \to 0$.

(d) $E > 0$, $F > 0$: These orbits are unbounded outward, but bounded inward by $r \geq R = \sqrt{F/E}$. The results are identical to case (a), except for a change of signs of E and F:

$$r = \frac{R}{\left| \cos \int_{\theta_0}^{\theta} \frac{\sqrt{F}d\theta}{\sqrt{F - f(\theta)}} \right|} , \tag{32}$$

$$t = \pm R/\sqrt{2E/m} \tan \int_{\theta_0}^{\theta} \frac{\sqrt{F}d\theta}{\sqrt{F - f(\theta)}} . \tag{33}$$

If one starts at $r = R$, the particle spirals out in either direction. The particle leaves the system on an asymptotic straight line when the argument to the cosine in the denominator equals $\pi/2$.

(e) $E > 0$, $F = 0$: This is also a special case,

$$r = |R \pm \sqrt{2E/m}\, t| , \tag{34}$$

$$r = \frac{R}{\left| 1 \pm R \int_{\theta_0}^{\theta} \frac{\sqrt{E}d\theta}{\sqrt{-f(\theta)}} \right|} . \tag{35}$$

Once again, this result can be derived from (d) by shifting the time and angle origin and taking $F \to 0$. R is a given initial radius.

(f) $E > 0$, $F < 0$: Define, $F = -ER^2$. Changing R^2 to $-R^2$ in Eq. (25)

$$r = \sqrt{|(2E/m)t^2 - R^2|} , \tag{36}$$

the orbit is found to be

$$r = \frac{R}{\left| \sinh\left(\sinh^{-1}(1) \pm \int_{\theta_0}^{\theta} \frac{\sqrt{-F}d\theta}{\sqrt{F - f(\theta)}} \right) \right|} . \tag{37}$$

Except for cases (a) and (b), all orbits are unbounded. Among these unbounded orbits, only (d) has a nonzero lower bound on the radius; the rest can reach the center of the potential. Figure 3 shows the classification of orbits in terms of E and F, and gives examples of orbits of type (a), (d), and (f). Type (b) is at the origin of the $E \sim F$ plane; type (c) is on the negative F axis, and type (e) is on the positive E axis. Examples of orbits of types (c) and (e) are shown in Fig. 4.

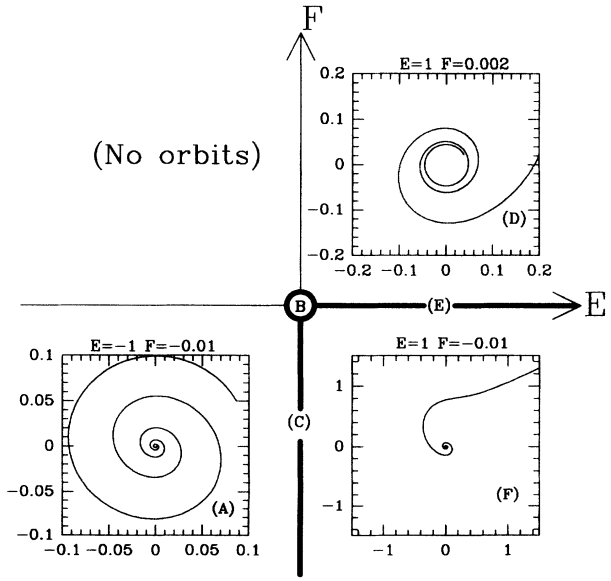

FIG. 3. Classification of orbits for the inverse-square potential in terms of conserved quantities E and F. Types (d), (a), and (f) appear in the first, the third, and the fourth quadrants; examples of orbits are shown. There are no orbits allowed in the second quadrant. Type (b), the circular orbit, appears only at the origin of $E \sim F$ plane. Examples for type (c) (on the negative F axis), type (e) (on the positive E axis), are shown in Fig. 4.

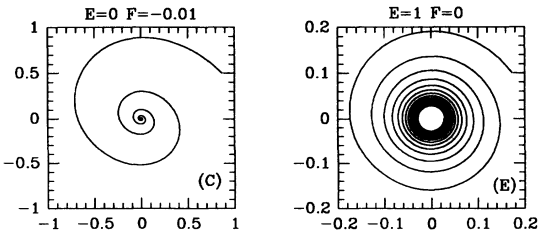

FIG. 4. Examples of type (c) and (e) orbits.

IV. THE VORTICITY OF THE PROBABILITY FIELD

From the last section, we know that an orbit near the center of a quantum vortex is a circle. This makes a study of the vortex properties for small r very easy. For a circular orbit of radius R, it is found that

$$\dot{\theta} = \frac{\hbar ab}{mR^2(b^2\cos^2\theta + a^2\sin^2\theta)} \quad , \tag{38}$$

and from this, the magnitude of the current density

$$j = \rho v = \hbar R/(mab) \tag{39}$$

is a constant. Along the circle, the velocity changes. This results in compression and decompression of the flow, causing the density to oscillate.

Knowing the velocity along a circle, we may calculate the the action

$$\oint \mathbf{p}\cdot d\mathbf{r} = \pm h \quad , \tag{40}$$

where the $\pm$ sign gives the direction of the circulation of the vortex; $+$ for right handed, and $-$ for left handed. Equation (40) is true for any closed curve enclosing a quantum vortex because $\nabla\times\mathbf{p}$ is zero everywhere else. Therefore,

$$\nabla\times\mathbf{p} = h\sum_i \Gamma_i\delta(\mathbf{r}-\mathbf{r_i}) \ , \tag{41}$$

where $\mathbf{r_i}$ is the location of a vortex, and $\Gamma_i = \pm 1$ accounts for the vortex chirality. This is equivalent to saying

$$\oint \mathbf{p}\cdot d\mathbf{r} = (N_+ - N_-)h \tag{42}$$

for any simple closed contour, where $N_\pm$ are the numbers of right and left handed vortices enclosed. Such a contour must be continuously contractable to a single point in the region where the wave function is defined, i.e., there can be no holes in it. The requirement that the action along any closed curve be an integer multiple of Planck's constant ensures that the wave function is single valued.

Let us now add on a magnetic field. The force generated by the quantum potential is proportional to $1/r^3$, while the velocity of the particle, and thus the Lorentz force, is of the order of $1/r$. Just like V, it can be neglected for small r. Thus,

$$\nabla\times\mathbf{p} = h\sum_i \Gamma_i\delta(\mathbf{r}-\mathbf{r}_i) - q\mathbf{B} \tag{43}$$

and

$$\oint \mathbf{p}\cdot d\mathbf{r} + q\Phi = (N_+ - N_-)h \ , \tag{44}$$

where Φ is the flux passing through the enclosed surface. This formula quantizes the sum of the action along a closed path and the charge times the flux enclosed, in terms of the number of quantum vortices.

V. GENERALIZATION TO THREE-DIMENSIONAL SPACE

In this section, we discuss quantum vortices and vorticity of the probability field in three-dimensional space. As in the previous sections, we first discuss the situation where $\mathbf{B}$ is absent. When the wave function is nonzero, $\nabla\times\mathbf{p} = 0$; the field is irrotational. The interesting points are those where $\rho = 0$. First, let's discuss an isolated wave function node. Assume $\mathbf{r_0}$ is an isolated node, $\rho(\mathbf{r_0}) = 0$, $\rho(\mathbf{r_0}+\boldsymbol{\epsilon}) > 0$, where $\boldsymbol{\epsilon}$ is an arbitrary small vector. We wish to see if any quantum vortex can form around this node. Choosing any small closed path around the node, we can compute the action $\oint \mathbf{p}\cdot d\mathbf{r}$. However, since the node is isolated, one can always find a surface with the path as its boundary, and evading the singular point. Since $\nabla\times\mathbf{p}$ is zero on the surface, the action along the path is zero. Thus, no quantum vortex will form around an isolated wave function node in three-dimensional space. For completeness, the classical solution for a particle in three-dimensional inverse-square potential is given in Appendix A.

The proper place to see a quantum vortex in three-dimensional space is where wave function nodes form a continuous curve, either closing on itself or ending on the boundary (which also consists of wave function nodes). This requirement breaks down the condition which results in vanishing action around a closed path winding a nodal line. The reason is that for any surface with the path as its boundary, there must be at least one singular point where the nodal line crosses the surface. Actually, for a short enough path, there will be only one singular point. Now let $\mathbf{r_0}$ be one of the points on a closed nodal curve, and consider a small enough neighborhood so that the nodal curve can be considered to be a straight line segment. Taking a plane orthogonal to the curve, one can establish a local cylindrical coordinate system. Bearing in mind that the wave function magnitude must be nonnegative, the Taylor expansion of ρ is independent of z, and depends quadratically on r. The quantum potential is then also independent of z, but an inverse square function of r. Thus, on the plane orthogonal to the nodal curve, the previous two-dimensional discussion applies. Thus, stream lines close to a nodal curve are circles in planes perpendicular to it. The sheets of flow around the nodal curve form concentric tori; they are like long concentric cylinders bent to close at the ends.

Now suppose $\mathbf{r}_i$ are the coordinates of the nodal curves,

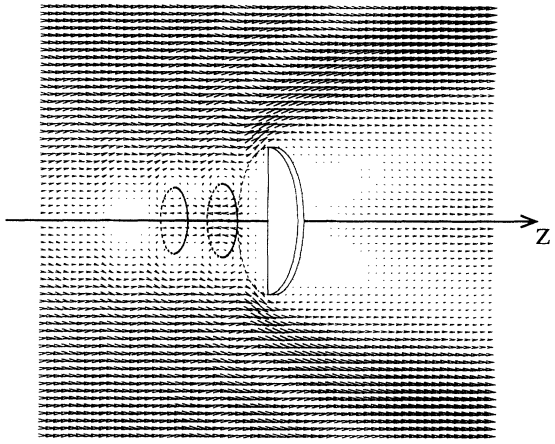

FIG. 5. Three-dimensional scattering problem for a thin hard disk of radius R. Z is taken to be the symmetry axis, and the beam is parallel to it. Flux density field is plotted in one plane including the symmetry axis. Two nodal curves are plotted, and they are circles with Z as their symmetry axis. Vortices form about the nodal curve due to backward scattering from the target, giving a flow in the negative Z direction inside the nodal curve. The energy of the beam is $E = 5\hbar^2/(2mR^2)$.

then the vorticity of the probability field is

$$\nabla \times \mathbf{p} = h \sum_i \oint \delta(\mathbf{r} - \mathbf{r}_i) d\mathbf{r}_i \ , \tag{45}$$

where the closed path line integral is taken in the direction determined by the rotation of the vortex using the right hand rule. When a magnetic field is present, a $-q\mathbf{B}$ term should be added. Finally, the action-flux-quantum vortex relation is the same as for the two-dimensional case. As an illustration of quantum vortex in three-dimensional space, consider an identical particle beam of energy E scattering from a thin hard disk of radius R. Let the beam be normal to the surface of the disk. When the energy of the beam is small, no vortex is seen. As the energy rises, vortices build up in the region of backward scattering due to strong interference between the incident and scattered waves. Figure 5 plots the flux density field ($\mathbf{j}$) in a plane containing the symmetry axis Z. Two vortices are seen, associated with the nodal curves which are circles perpendicular to the symmetry axis.

VI. CONCLUSION

In this paper, we have derived the inverse-square quantum potential near a wave function node, based on Bohm's prescription. The corresponding classical problem was then solved, and possible orbits classified. It was proved that the only possible closed orbits in two dimensions are circles, and thus stream lines near the center of a quantum vortex are circles. Based on the properties of a quantum vortex, the vorticity of the probability flow was found. Its integral form gives a relation between the action, the flux and the number of vortices associated with a closed path. This relationship was also generalized to the three-dimensional case, in which a closed wave function nodal curve replaces the point node of two-dimensional space. Work is on going to study the possible connections of quantum vortices with flow turbulence, and the quantum potential with quantum chaos research.

ACKNOWLEDGMENTS

We are grateful to NSERC Canada for continued support under research Grant No. OGP00-3198. We thank Dr. C. R. Leavens for reminding us Bohm's interpretation of quantum mechanics and its relevance to probability flux. We also thank Professor J. Carbotte for pointing out the connection between superconductivity theory and the present work.

APPENDIX A: CLASSICAL SOLUTION TO THE THREE-DIMENSIONAL INVERSE-SQUARE POTENTIAL

In spherical coordinates, the three-dimensional inverse-square potential is

$$V = f(\theta, \phi)/r^2 \tag{A1}$$

and the Lagrangian is

$$L = \frac{1}{2}(\dot{r}^2 + r^2\dot{\theta}^2 + r^2 \sin^2\theta\dot{\phi}^2) - \frac{f(\theta,\phi)}{r^2} \ , \tag{A2}$$

which results in differential equations of motion

$$m\ddot{r} = mr(\dot{\theta}^2 + \sin^2\dot{\phi}^2) + 2f(\theta,\phi)/r^3 \ , \tag{A3}$$

$$\frac{d}{dt}(mr^2\dot{\theta}) = m\sin\theta\cos\theta R^2\dot{\phi}^2 - \frac{1}{r^2}\frac{\partial f}{\partial\theta} \ , \tag{A4}$$

and

$$\frac{d}{dt}(mr^2\sin^2\theta\dot{\phi}^2) = -\frac{1}{r^2}\frac{\partial f}{\partial\phi} \ . \tag{A5}$$

Combining $\dot{\theta}r^2\times$(A4)$+\dot{\phi}r^2\times$ (A5), and moving everything from the right to the left,

$$\frac{d}{dt}\left[\frac{1}{2}mr^4(\dot{\theta} + \sin^2\theta\dot{\phi}^2) + f(\theta,\phi)\right] = 0 \ . \tag{A6}$$

Therefore, just as for the two-dimensional inverse-square potential,

$$F = r^2\left(E - \frac{1}{2}m\dot{r}^2\right) \tag{A7}$$

is a conserved quantity. This implies that $r(t)$ takes the same form as in the two-dimensional case. The solution for $\theta(t)$, $\phi(t)$ depends on the specific form of $f(\theta,\phi)$. As in the two-dimensional case, if there are closed orbits,

they must obey $E = F = \dot{r} = 0$. In other words, closed orbits are only possible on spheres. However, the theory does not guarantee their existence.

APPENDIX B: SOLUTION TO THE THIN HARD DISK SCATTERING PROBLEM

The problem is to solve the Helmholz equation

$$\nabla^2\Psi + k^2\Psi = 0 \ , \tag{B1}$$

with $\Psi = 0$ on the disk. For $r > R$, the solution takes the form

$$\Psi = \frac{1}{kr}\sum_l i^l(2l+1)[j_l(jr) + \alpha_l h_l^{(1)}(kr)]P_l(\cos\theta) \ . \tag{B2}$$

If all α_l were zero, this would reduce to the plane wave expansion for the incoming beam.

For $r < R$, since the wave function vanishes on the disk surface ($\theta = \pi/2$), only odd angular momentum partial waves are needed,

$$\Psi = \frac{1}{kr}\sum_{l\in odd} \beta_l i^l(2l+1)j_l(kr)P_l(\cos\theta), \quad \cos\theta > 0 \tag{B3}$$

$$\Psi = \frac{1}{kr}\sum_{l\in odd} \gamma_l i^l(2l+1)j_l(kr)P_l(\cos\theta), \quad \cos\theta < 0 \ . \tag{B4}$$

Matching the wave function at $r = R$ results in

$$\beta_l = \frac{j_l + \alpha_l h^{(1)}}{j_l} + \sum_{n\in even} i^{n-l}(2n+1)\frac{j_n + \alpha_n h^{(1)}}{j_l} I_{nl} \ , \tag{B5}$$

$$\gamma_l = \frac{j_l + \alpha_l h^{(1)}}{j_l} - \sum_{n\in even} i^{n-l}(2n+1)\frac{j_n + \alpha_n h^{(1)}}{j_l} I_{nl} \ , \tag{B6}$$

where the Bessel function take argument kR and

$$I_{nl} = \int_0^1 P_n(x)P_l(x)dx = \frac{l(-1)^{(n+l-1)/2}(n-1)!!(l-2)!!}{[l(l+1) - n(n+1)]n!!(l-1)!!} \ . \tag{B7}$$

Furthermore, matching the normal derivative of the wave function at $r = R$ results in

$$\alpha_l = 0 \ \text{ for odd } l \ , \tag{B8}$$

while

$$\sum_{n\in even}[C_{mn}i^n(2n+1)h^{(1)} - i^m h_m'^{(1)}\delta_{mn}]\alpha_n = i^m j_m' - \sum_{n\in even} C_{mn}i^n(2n+1)j_n \tag{B9}$$

for non-negative even integers n and m, where

$$C_{mn} = \sum_{l\in odd}(2l+1)I_{ml}I_{nl}j_l'/j_l \ . \tag{B10}$$

Solving Eq. (B9) gives solutions for the α_n of the even partial waves.

[1] Hua Wu and D. W. L. Sprung, Phys. Lett. A **183**, 413 (1993).

[2] D. Bohm, Phys. Rev. **85**, 166 (1952); **85**, 180 (1952).

[3] D. Bohm, B. J. Hiley, and P. N. Kaloyerou, Phys. Rep. **144**, 321 (1987).

[4] R. P. Feynman, R.B. Leighton, and M. Sands, in *The Feynman Lectures on Physics* (Addison-Wesley, New York, 1965), Vol. 3, Chap. 21.

[5] F. Calogero, J. Math. Phys. **10**, 2191 (1969); **10**, 2197 (1969).

[6] B. Sutherland, J. Math. Phys. **12**, 246 (1971); **12**, 251 (1971); Phys. Rev. A **4**, 2019 (1971).

[7] B. S. Shastry and B. Sutherland, Phys. Rev. Lett. **70**, 4029 (1993).

[8] B. D. Simons, P. A. Lee, and B. L. Altshuler, Phys. Rev. Lett. **70**, 4122 (1993).

[9] B. Sutherland and B. S. Shastry, Phys. Rev. Lett. **71**, 5 (1993).

[10] P. Exner, P. Šeba, and P. Šťovíček, Czech. J. Phys. B **39**, 1181 (1989).

[11] J. Martorell, S. Klarsfeld, D. W. L. Sprung, and H. Wu, Solid State Commun. **78**, 13 (1991).

[12] Hua Wu, D. W. L. Sprung, and J. Martorell, Phys. Rev. B **45**, 11 960 (1992).

[13] Hua Wu, D. W. L. Sprung, and J. Martorell, J. Appl. Phys. **72**, 151 (1992).

[14] Hua Wu and D. W. L. Sprung, Phys. Rev. B **47**, 1500 (1993).